Int. J. Cancer: **118,** 821–831 (2006)
© 2005 Wiley-Liss, Inc.

Loss of intercellular adhesion activates a transition from low- to high-grade human squamous cell carcinoma

Alexander Margulis[1], Weitian Zhang[1], Addy Alt-Holland[1], Sujata Pawagi[2], Padmaja Prabhu[2], Jian Cao[3], Stanley Zucker[3,4], Laurence Pfeiffer[2], Jacqueline Garfield[5], Norbert E. Fusenig[6] and Jonathan A. Garlick[1]*

[1]*Division of Cancer Biology and Tissue Engineering, Department of Oral and Maxillofacial Pathology, School of Dental Medicine, Tufts University, Boston, MA, USA*
[2]*Department of Oral Biology and Pathology, State University of New York at Stony Brook, Stony Brook, NY, USA*
[3]*Department of Medicine, State University of New York at Stony Brook, Stony Brook, NY, USA*
[4]*Department of Veterans Affairs Medical Center, Northport, NY, USA*
[5]*LifeCell Inc., Branchburg, NJ, USA*
[6]*German Cancer Research Center, Heidelberg, Germany*

The relationship between loss of intercellular adhesion and the biologic properties of human squamous cell carcinoma is not well understood. We investigated how abrogation of E-cadherin-mediated adhesion influenced the behavior and phenotype of squamous cell carcinoma in 3D human tissues. Cell-cell adhesion was disrupted in early-stage epithelial tumor cells (HaCaT-II-4) through expression of a dominant-negative form of E-cadherin (H-2K^d-Ecad). Three-dimensional human tissue constructs harboring either H-2K^d-Ecad-expressing or control II-4 cells (pBabe, H-2K^d-EcadΔC25) were cultured at an air-liquid interface for 8 days and transplanted to nude mice; tumor phenotype was analyzed 2 days and 2 and 4 weeks later. H-2K^d-Ecad-expressing tumors demonstrated a switch to a high-grade aggressive tumor phenotype characterized by poorly differentiated tumor cells that infiltrated throughout the stroma. This high-grade carcinoma revealed elevated cell proliferation in a random pattern, loss of keratin 1 and diffuse deposition of laminin 5 γ2 chain. When II-4 cell variants were seeded into type I collagen gels as an *in vitro* assay for cell migration, we found that only E-cadherin-deficient cells detached, migrated as single cells and expressed N-cadherin. Function-blocking studies demonstrated that this migration was matrix metalloproteinase-dependent, as GM-6001 and TIMP-2, but not TIMP-1, could block migration. Gene expression profiles revealed that E-cadherin-deficient II-4 cells demonstrated increased expression of proteases and cell-cell and cell-matrix proteins. These findings showed that loss of E-cadherin-mediated adhesion plays a causal role in the transition from low- to high-grade squamous cell carcinomas and that the absence of E-cadherin is an important prognostic marker in the progression of this disease.
© *2005 Wiley-Liss, Inc.*

Key words: E-cadherin; squamous cell carcinoma; matrix metalloproteinase; laminin 5; tumor microenvironment

E-cadherin is known to be a tumor suppressor gene since the loss of E-cadherin function in tumor progression during the advanced stages of carcinoma progression is well established[1–3] and has been linked to a poor clinical prognosis *in vivo*.[4–6] Studies using 2D monolayer cultures have demonstrated the direct influence of E-cadherin function on the malignant properties of transformed cells at an advanced stage. For example, abrogation of E-cadherin-mediated adhesion[7–10] induced tumor cell invasion *in vitro* while restoration of E-cadherin function resulted in growth retardation and inhibition of invasive properties.[3,9] However, the role that loss of E-cadherin-mediated adhesion may play in early stages of carcinoma progression is poorly understood, as studies have demonstrated either a reduction[11,12] or an increase[13,14] of E-cadherin function during the initial stages of epithelial cancer progression.

Further elucidation of the impact of altered cell-cell adhesion on early events in squamous cell carcinoma progression has been limited by the inability of monolayer culture to replicate fully the biologically meaningful pathways that couple cell-cell adhesion and growth that occur *in vivo*.[15] The need for 3D tissue models has become even more apparent in recent years due to the emerging view that the tumor cell microenvironment plays an important role in the control of neoplastic progression through a dynamic reciprocity between tumor cells and their surrounding tissues. Since cell-cell adhesion is intimately linked to tissue organization, the impact of the abrogation of E-cadherin-mediated adhesion on cancer progression needs to be studied in 3D tissue context to represent more accurately early events as they occur in human tissues *in vivo*. To accomplish this, we have previously developed 3D, human tissue models of stratified squamous epithelium that mimic the architectural features of the premalignant stage of squamous cell carcinoma.[16–18] These tissue constructs have been generated with a well-characterized keratinocyte cell line (HaCaT-II-4), which formed invasive tumors with a low-grade malignant behavior after surface transplantation to nude mice.[16,19,20] This cell line represents an early stage of transformation to squamous cell carcinoma and is well-suited for incorporation into models of early stages of tumor progression.[21]

It remains unclear how alterations in E-cadherin-mediated adhesion are directly linked to the biologic behavior of squamous cell carcinoma *in vivo*. To address this, we have characterized the impact of loss of E-cadherin function on the behavior of human squamous cell carcinoma cells manifesting a low-grade biologic behavior in bioengineered 3D tissues grown *in vivo*. We found that loss of adherens junctions (AJs) upon disruption of E-cadherin function significantly accelerated tumorigenesis through the induction of a switch to an aggressive high-grade tumor phenotype when these tissues were transplanted to nude mice. Immunohistochemical and ultrastructural analyses of these tumors revealed that activation of this high-grade behavior was associated with loss of differentiation, altered laminin 5 deposition and a dramatic increase in cell proliferation. Additionally, only E-cadherin-deficient II-4 cells detached and migrated as single cells in a 3D collagen matrix model of invasion and demonstrated cadherin switching to N-cadherin upon loss of E-cadherin. Function-blocking studies demonstrated that migration of E-cadherin-deficient II-4 cells in collagen matrices was matrix metalloproteinase (MMP)-dependent, as GM-6001 and TIMP-2, but not TIMP-1, could block cell migration. Microarray analysis revealed elevated expression of active genes that mediate survival-signaling pathways, extracellular matrix proteolysis and cell-cell and cell-matrix adhesion. These findings demonstrate a causal link between loss of E-cadherin-mediated adhesion and a switch from low- to high-grade squamous cell carcinoma (SCC). This suggests that E-cadherin is an important prognostic marker whose absence is associated with a highly aggressive form of SCC.

Grant sponsor: the National Institutes of Dental and Craniofacial Research; Grant number: 2RO1DE011250-06.

***Correspondence to:** Division of Cancer Biology and Tissue Engineering, South Cove, Room 116, 55 Kneeland Street, Tufts University, Boston, MA 02111. Fax: +617-636-2915. E-mail: jonathan.garlick@tufts.edu

Received 10 January 2005; Accepted after revision 10 May 2005
DOI 10.1002/ijc.21409
Published online 8 September 2005 in Wiley InterScience (www.interscience.wiley.com).

Material and methods

Monolayer (2D) cell culture

In preparation for the generation of 3D cultures, the HaCaT-*ras*-II-4 (II-4) cell line[19–21] was transduced with retroviral constructs described below and grown in 2D monolayer culture in Dulbecco's modified Eagle's medium (DMEM) containing 5% fetal calf serum. 293 Phoenix cells used for production of retroviral vectors were maintained in DMEM containing 10% bovine calf serum while human dermal fibroblasts used in 3D cultures were derived from newborn foreskins and grown in media containing DMEM and 10% fetal calf serum. All cells were grown at 37°C, 7.5% CO_2.

Retroviral infections

293 Phoenix producer cells were transfected with pBabe, pBabe-H-2K^d-Ecad or pBabe-H-2K^d-EcadΔC25 plasmids (gifts from Dr. F. Watt, Imperial Cancer Research Center, London, U.K.) by the calcium phosphate method. Transfected cells were grown at 32°C and viral supernatants were collected 48 hr later and used to infect II-4 cells in the presence of 4 μg/ml polybrene for 3 hr at 32°C. These target cells were maintained under puromycin selection (5 mg/ml) for 2 weeks starting 2 days postinfection.

Generation of 3D in vitro *constructs of stratified squamous epithelium and their* in vivo *transplantation*

Three-dimensional constructs were prepared *in vitro* as previously described.[18] Briefly, early-passage human dermal fibroblasts were added to neutralized type I collagen (Organogenesis, Canton, MA) to a final concentration of 2.5×10^4 cells/ml; 3 ml of this mixture was added to each 35 mm well insert of a 6-well plate and incubated for 4–6 days in media containing DMEM and 10% fetal calf serum until the collagen matrix showed no further shrinkage. Cells were seeded directly on a deepidermalized dermis derived from human skin (AlloDerm; LifeCell, Branchburg, NJ), which was layered on the contracted collagen gel described above to enable fibroblasts to migrate and repopulate the AlloDerm from below. A total of 5×10^5 cells were seeded on the surface of the AlloDerm. Cultures were maintained submerged in low calcium epidermal growth media for 2 days, submerged for 2 days in normal calcium epidermal growth media and raised to the air-liquid interface by feeding from below for 7 days. For *in vivo* transplantation of these 3D constructs, 6-week-old male Swiss nude mice (N:NIHS-nuf DF; Taconic Farms, Germantown, NY) were anesthetized using xylazine:ketamine (1:1) and a 1.3 cm dorsal skin was removed. Three-dimensional constructs were placed onto fascia at the site of skin excision, covered with petrolatum gauze (Sherwood Pharmaceuticals, St. Louis, MO) and secured with bandages (Baxter Scientific). Bandages were changed every 3–4 days and removed after 2 weeks. Animals were sacrificed 4 days, 2 weeks and 4 weeks after transplantation and specimens were excised with underlying fascia. Tumor volume was measured at this time using a digital calipers and was estimated using the formula $V = L \times W \times H$, where L is the length, H is the height and W is the width of the tumor. Animals were grafted in triplicate for each time point.

3D collagen gel migration assay

H-2K^d-Ecad-, pBabe-, or H-2K^d-Ecad-ΔC25-expressing II-4 cells were added to neutralized type I collagen (Organogenesis) to a final concentration of 1.0×10^5 cells/ml; 3 ml of this mixture was added to each 35 mm well insert of a 6-well plate and incubated for 7 days in media containing DMEM and 5% fetal calf serum. At this time, collagen gels were grown at an air-liquid interface and exposed to either recombinant TIMP-1 (200 ng/ml) or TIMP-2 (200 ng/ml; Chemicon, Temecula, CA) or GM-6001 (10 μM; EMD Bioscience, La Jolla, CA) in serum-free media for an additional 4 days. Tissues were bisected and one-half of the specimen was formalin-fixed, paraffin-embedded and stained by hematoxylin and eosin stain while the other half was snap-frozen in liquid nitrogen and used for immunohistochemical staining.

Microarray analysis

II-4 cells expressing the empty vector (pBabe) or the H-2K^d-Ecad fusion protein were seeded at a density of 2×10^5 cells on type IV collagen-coated 6-well plates (BD Biosciences, Bedford, MA). Cells were grown for 24 hr in media containing DME and 5% FBS, washed twice with serum-free media and maintained in serum-free media for an additional 24 hr. RNA was extracted using RNeasy Mini Kit (Qiagen, Valencia, CA) according to the manufacturer's protocol. Synthesis of aminoallyl-dUTP-labeled first-strand cDNA was performed with 15 μg total RNA using SuperScript II reverse transcriptase, Oligo(dT) 12-18 primers (Invitrogen, Carlsbad, CA), as recommended by the manufacturer. cDNA was then purified using G-50 columns (Amersham, Piscataway, NJ), concentrated by speedvac and labeled with Cy5 (pBabe) or Cy3 (H-2K^d-Ecad) dyes (Amersham) for 1 hr at room temperature. Labeled cDNA was purified by GFX column (Amersham) and incubated with H21K and H6K arrays (prepared in Tufts-New England Medical Center Expression Array Core) in hybridization buffer (Amersham) with 50% formamide for 2 days at 42°C. Slides were washed once with $1 \times$ SSC plus 0.2% SDS for 10 min, twice with $0.1 \times$ SSC plus 0.2% SDS for 10 min and 4 times with $0.1 \times$ SSC for 30 sec and then scanned using a Scanarray 4000 scanner (Perkin Elmer, Fremont, CA). Images were analyzed by Imagene software (BioDiscovery, Marina Del Rey, CA) and the ratio of 2 fluorescence intensities for control, pBABE- and H-2K^d-Ecad-expressing II-4 cells were calculated for each spot. Data were then normalized using Genespring software (Agilent Technologies, Redwood City, CA).

Immunofluorescence

Excised tumors were frozen in embedding media (Triangle Biomedical, Durham, NC) in liquid nitrogen vapors after being placed in 2 M sucrose for 2 hr at 4°C. Tissues were serial-sectioned at 6 μm and mounted onto gelatin-chrome alum-coated slides. Tissue sections were washed with PBS, blocked with 10 μg/ml goat IgG, 0.05% goat serum and 0.2% BSA vol/vol in PBS. Cells or tissues were then stained with mouse anti-β-catenin (BD Pharmingen Transduction Labs, Lexington, KY), mouse anti-E-cadherin (HECD-1, against extracellular domain; Zymed, South San Francisco, CA), mouse antikeratin 1 (Enzo Diagnostics, Farmingdale, NY), rabbit anti-N-cadherin (Sigma, St. Louis, MO) and rabbit antilaminin 5 γ2 chain (gift from Dr. G. Meneguzzi, Nice, France). Immunoreactive proteins were detected using Alexa 488-conjugated goat antirabbit or Alexa 594-conjugated goat antimouse IgG (Molecular Probes, Eugene, OR). Fluorescence was visualized using a Nikon OptiPhot microscope and single- or double-exposure photomicroscopy was performed using either FITC or Texas Red filters, or both. For routine light microscopy, tissues were fixed in 10% neutral buffered formalin and embedded in paraffin; 4 μm sections were stained with hematoxylin and eosin. Ki-67 staining was performed using paraffin-embedded sections that were deparaffinized and stained with a mouse anti-Ki-67 antibody after antigen retrieval with sodium citrate.

Transmission electron microscopy

Four days after transplantation, grafts were excised and cut into pieces of approximately 2×2 mm, fixed in 2% glutaraldehyde in 0.1 M cacodylate and 0.1 M sucrose at pH 7.2 and postfixed in 2% osmium tetroxide in 0.1 M cacodylate and 1% tannic acid in 0.1 M cacodylate. Tissue samples were then dehydrated in graded ethanol, cleared with propylene oxide and infiltrated with Spurr's resin. Following polymerization of the resin, thick sections were produced using a Reichert Ultracut E microtome and sections were stained with toluidine blue to determine orientation. The blocks were then thin-sectioned at approximately 90 nm and mounted on copper grids. Grids were stained with 5% uranyl ace-

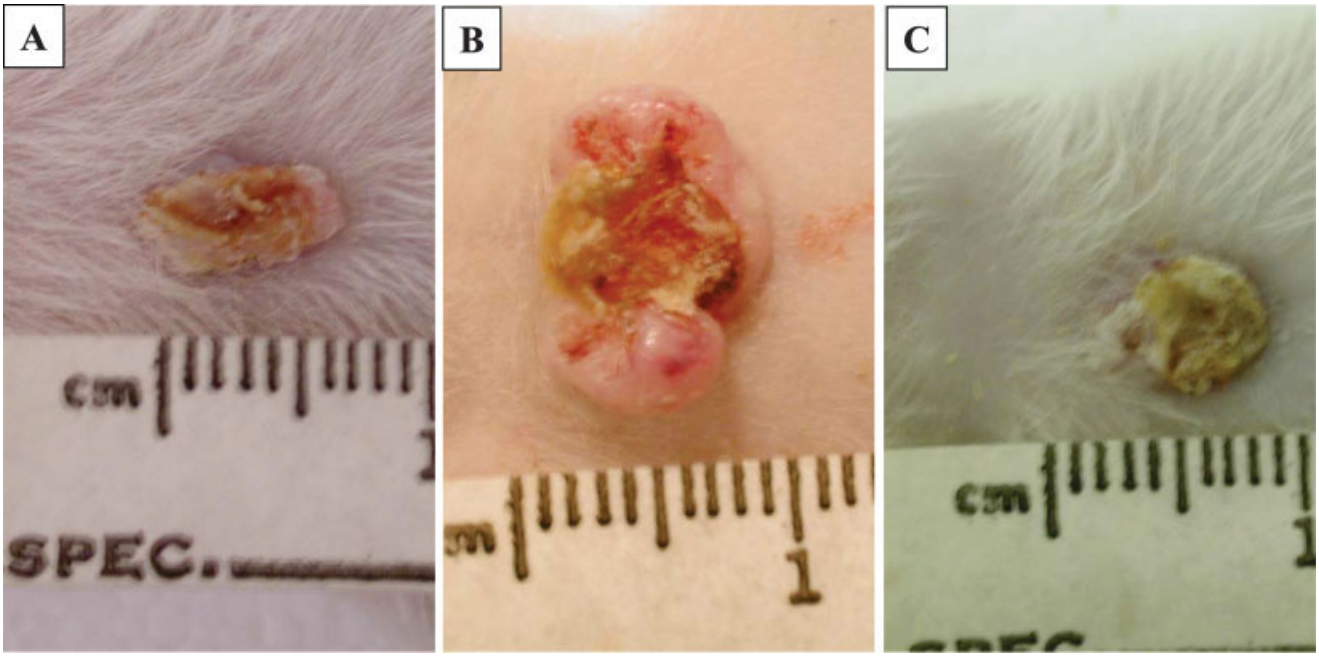

FIGURE 1 – Loss of E-cadherin function induces highly aggressive tumors after transplantation of II-4 cells. Four weeks after grafting, H-2K^d-Ecad-expressing II-4 cells formed large nodular tumors with central areas of ulceration (*b*). II-4 cells expressing either pBabe (*a*) or H-2K^d-EcadΔC25 (*c*) formed considerably smaller tumors that appeared as slightly raised hyperkeratotic plaques.

tate in deionized water and Reynold's lead citrate and were examined at various magnifications using a Hitachi H-600 transmission electron microscope.

Results

Suppression of E-cadherin function activates a switch to a high-grade aggressive carcinoma

II-4 cells were infected with a dominant-negative E-cadherin retroviral construct expressed in a pBabe-puro vector (H-2K^d-Ecad). This vector contained the cytoplasmic and transmembrane portions of E-cadherin and the extracellular domain of H-2K^d and was previously shown to abrogate cell adhesion in primary keratinocytes.[22] As control vectors, we used H-2K^d-EcadΔC25, a fusion protein identical to H-2K^d-Ecad except for a 25 amino acid deletion in its β-catenin binding domain and an empty pBabe-puro vector. II-4 cells were transduced with these 3 vectors, grown *in vitro* at an air-liquid interface for 7 days to generate well-stratified 3D tissue constructs and transplanted as surface grafts to nude mice. To determine the effect of E-cadherin loss on tumor progression, transplants were examined 2 and 4 weeks after grafting. Grafts generated with H-2K^d-Ecad-infected cells formed significantly larger tumors (Fig. 1*b*) than tissues comprised of II-4 cells expressing pBabe or H-2K^d-EcadΔC25 (Fig. 1*a* and *c*). The volume of these E-cadherin-deficient tumors was 9-fold greater than those of E-cadherin competent tumors when tumor volume was measured and compared 2 weeks after transplantation. These E-cadherin-deficient tumors demonstrated raised, nodular and erythematous tumor margins and a central area of ulceration, while control grafts appeared as hyperkeratotic plaques that were slightly raised above the surface. To determine the histologic appearance of these tumors during an earlier stage of tumor cell progression, transplants were examined 2 weeks after grafting. Tissues harboring pBabe and H-2K^d-EcadΔC25-expressing II-4 cells invaded into the underlying connective tissue as large well-differentiated tumor cell islands that were well demarcated from the surrounding connective tissue with central keratin pearls (Fig. 2*a*, *c*, *d* and *f*). Proliferating cells were found exclusively in basal cells at the edge of these tumor cell islands (Fig. 2*g* and *i*). Thus, these control tumors manifested the low-grade behavior that has been previously reported after transplantation of these cells.[16,21] In contrast, H-2K^d-Ecad-expressing tumor cells invaded into the underlying stroma as highly infiltrative, poorly differentiated cells (Fig. 2*b*) that migrated from the edge of the tumor as small clusters or as individual cells (Fig. 2*e*). These invading cells exhibited a significantly more aggressive pattern of invasion that was characterized by cell proliferation throughout the tumor mass in a random pattern (Fig. 2*h*).

Loss of cell-cell adhesion structures is associated with rapid disruption of basement membrane integrity

In order to assess the ultrastructural features of cell-cell adhesion structures and basement membrane organization in 3D transplants upon loss of E-cadherin function, grafted tissues were studied by transmission electron microscope (TEM) 4 days after transplantation (Fig. 3). At lower magnifications, tissues constructed with H-2K^d-EcadΔC25 showed normal intercellular adhesion structures (Fig. 3*a*, arrows) and widened intercellular spaces (Fig. 3*a*, asterisks inset) as previously described for II-4 cells.[23] Under higher magnification, well-formed desmosomes were found (Fig. 3*a*, inset), indicating that control II-4 cells retained their capacity to form these structures. In contrast, tissues harboring H-2K^d-Ecad-expressing cells showed a significant degree of tissue disorganization and loss of architecture that was accompanied by the complete loss of intercellular adhesion structures (Fig. 3*b*). Intercellular spaces demonstrated numerous interdigitating filopodial processes that spanned between adjacent cells to approximate each other, yet formed no contacts or adhesive structures (Fig. 3*b*, inset). These structures were reminiscent of pairs of filopodial extensions between adjacent keratinocytes that have previously been shown to represent an abortive attempt to form AJs.[24] Ultrastructural features of BM structure were also altered in H-2K^d-Ecad-expressing tissues and were characterized by a disrupted basement membrane (Fig. 3*d*) that showed focal remnants of hemidesmosomal structures adjacent to residual patches of lamina densa that were seen occasionally beneath H-2K^d-Ecad-expressing

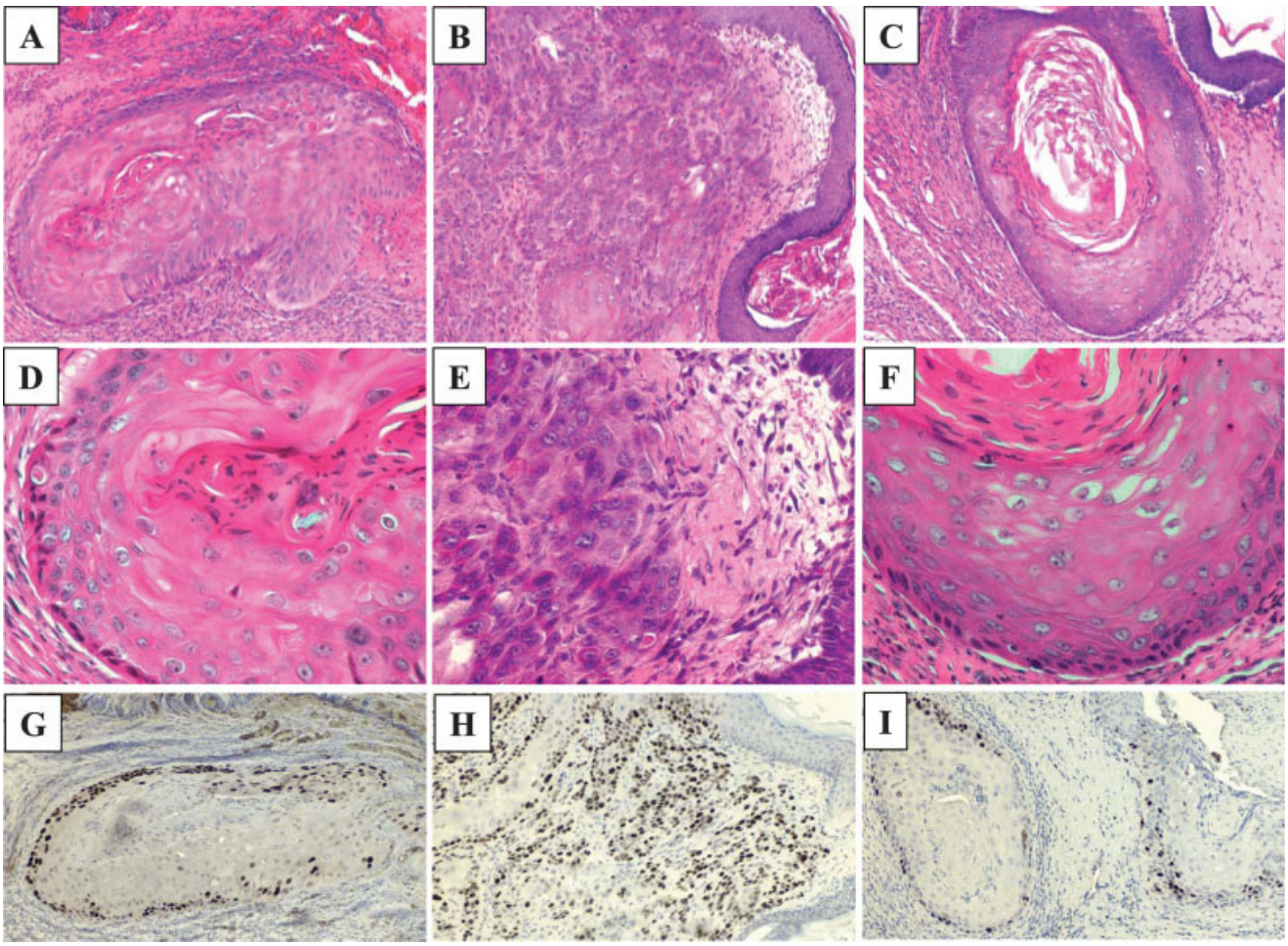

FIGURE 2 – II-4 cells exhibit a switch from low-grade tumors to highly invasive and proliferative high-grade tumors upon loss of E-cadherin function. Hematoxylin and eosin stain revealed that II-4 cells expressing pBabe (*a* and *d*) and H-2K^d-EcadΔC25 (*C* and *f*) demonstrated large well-differentiated islands of invasive tumor cells with central keratin pearls. In contrast, H-2K^d-Ecad-expressing II-4 cells (*b* and *e*) invaded as highly aggressive, poorly differentiated cells (*b*) that invaded as individual cells or as small clusters that migrated from the invasive edge (*e*). Staining with Ki-67 revealed that cells expressing H-2K^d-Ecad (*h*) proliferated throughout the tumor mass as well as in small clusters of cells budding from the leading invasive edge of the tumor. In contrast, pBabe- (*g*) and H-2K^d-EcadΔC25- (*i*) expressing control II-4 cells showed Ki-67 stain exclusively in basal cells at the periphery of large clusters. Original magnification: 10× (*a–c*); 40× (*d–f*); 10 × (*g–i*).

basal cells. In addition, individual cells extended filopodia into the superficial stroma in areas of basement membrane disruption (Fig. 3*e*). This was in contrast to the uninterrupted, well-formed BM structure seen in H-2K^d-EcadΔC25 transplants that included intact and linear lamina densa (Fig. 3*c*, inset). These findings demonstrated that complete loss of intercellular adhesion and disruption of basement membrane integrity were early events associated with abrogation of E-cadherin-mediated adhesion upon initiation of tumor cell invasion.

Switch to high-grade carcinoma upon loss of endogenous E-cadherin results in aberrant laminin 5 expression and loss of differentiation

To define the phenotype of high-grade tumors generated by H-2K^d-Ecad-expressing II-4 cells, 4-week transplants were analyzed by double immunohistochemical stain to determine the distribution of the γ2 chain of laminin 5 and either E-cadherin (Fig. 4*a–c*) or β-catenin (Fig. 4*d–f*). Control tumors expressing pBabe and H-2K^d-EcadΔC25 exhibited linear staining upon immunostaining with the γ2 chain of laminin 5 that was localized around the periphery of tumor cell islands (Fig. 4*a*, *c*, *d* and *f*). In contrast, H-2K^d-Ecad-expressing cells exhibited diffuse and pericellular distribution of γ2 chain (Fig. 4*b* and *e*). Loss of E-cadherin in these tumor cells was seen by the absence of this protein in H-2K^d-Ecad-expressing cells (Fig. 4*b*) and β-catenin was found in the cytoplasm of these cells (Fig. 4*e*), demonstrating that invasion was linked to redistribution of this protein component upon abrogation of E-cadherin-mediated adhesion. In contrast, pBabe- and H-2K^d-EcadΔC25-expressing II-4 cells demonstrated both E-cadherin (Fig. 4*a* and *c*) and β-catenin (Fig. 4*d* and *f*) in their normal intercellular distribution. Finally, differentiation status of the 4-week transplants was analyzed by double immunofluorescence stain for the differentiation marker keratin 1 and the γ2 chain of laminin 5. Transplants generated with control pBabe- and H-2K^d-EcadΔC25-expressing II-4 cells formed well-differentiated tumors, as seen by the strata-specific expression of keratin 1 in tumor cell islands that were surrounded by linear deposition of laminin 5 (Fig. 5*a* and *c*). In contrast, no keratin 1 expression was detected in tumors formed by H-2K^d-Ecad-infected cells (Fig. 5*b*), showing that loss of E-cadherin function was linked to truncation of the terminal differentiation program of these tumor cells. As described above, γ2 chain of laminin 5 was only seen in a pericellular distribution. Collectively, these results directly implicate the loss of E-cadherin-mediated adhesion in the switch from a well-differentiated to poorly differentiated carcinoma that accelerated

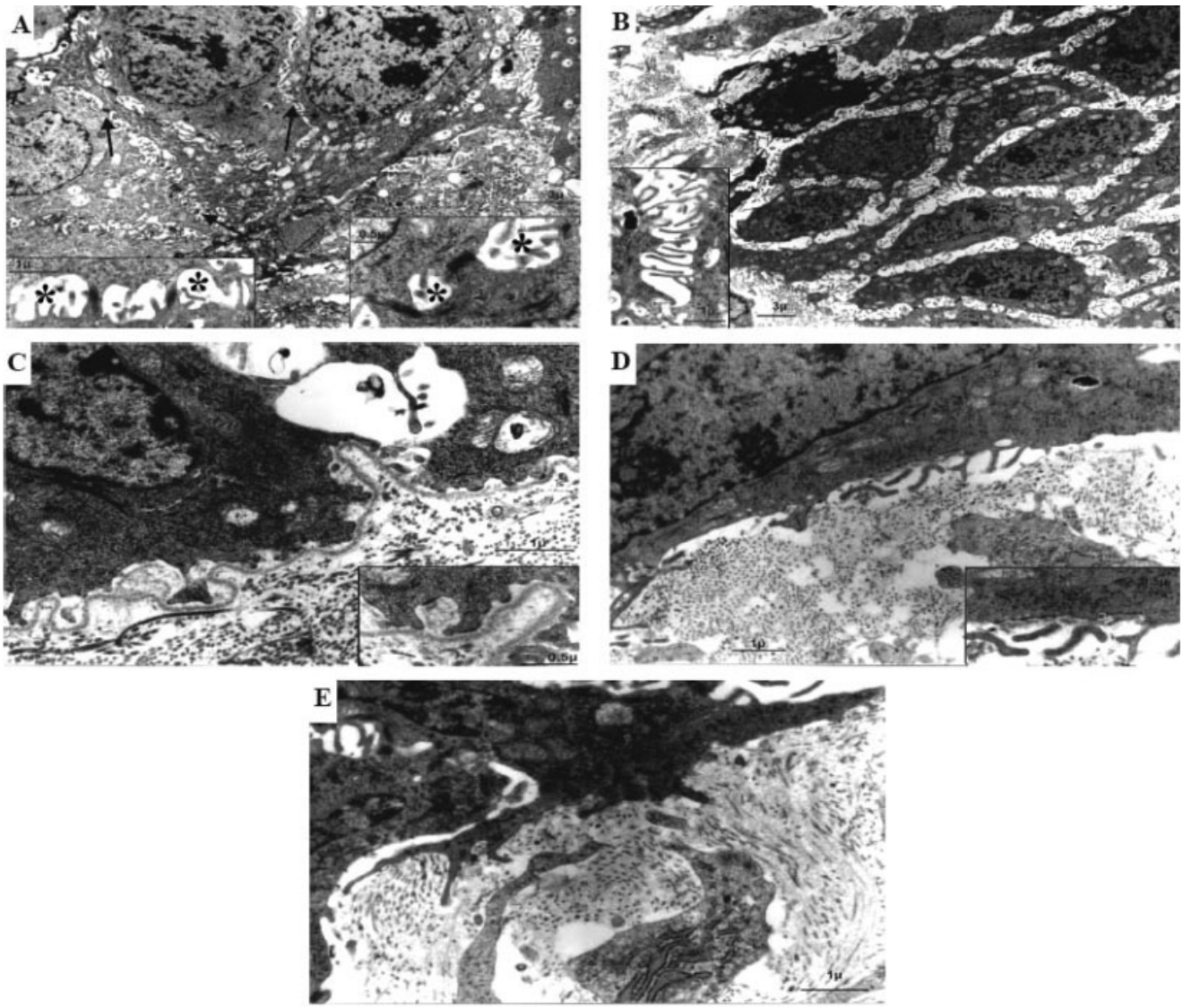

Figure 3 – Ultrastructural analysis reveals that loss of E-cadherin function in II-4 cells abolished cell-cell adhesion and disrupted basement membrane upon tumor cell invasion. Transplants of 3D constructs generated with H-2K^d-ΔC25-expressing controls (*a* and *c*) and dominant-negative E-cadherin-expressing II-4 cells (*b*, *d* and *e*) were examined by transmission electron microscopy 4 days postgrafting. Tissues generated with control II-4 cells demonstrated desmosomal structures (*a*, arrows) between widened intercellular spaces (*a*, inset, asterisks) and well-formed basement membrane as seen by the continuous lamina densa (*c*, inset). In contrast, II-4 cells expressing H-2K^d-Ecad completely lost cell-cell adhesion as seen by the absence of desmosomes (*b*) and showed numerous interdigitating filopodia at the cell-cell borders without any adhesive structures (*b*, inset). Basement membrane integrity was severely compromised as only focal remnants of lamina densa (*d*) were seen. Early invasion of H-2K^d-Ecad-expressing tumor cells demonstrated filopodia (*e*) that extended into the superficial stroma.

tumorigenesis through the generation of highly infiltrative and aggressive carcinomas.

E-cadherin-deficient cells activate MMP-mediated migration in 3D collagen gels

To understand mechanisms through which E-cadherin-deficient II-4 cells underwent accelerated invasion after *in vivo* transplantation, II-4 cell variants were seeded into type I collagen gels to generate a 3D *in vitro* assay for cell migration in a collagen matrix microenvironment. E-cadherin-competent control II-4 cell lines (H-2K^d-Ecad-ΔC25 and pBabe) generated round to ovoid cell clusters that were dispersed throughout the collagen gel (Fig. 6*a*, panels A and C). Under higher magnification, these clusters demonstrated polarized cells at their periphery that did not separate from adjacent cells and did not migrate into the surrounding collagen (Fig. 6*a*, panels D and F). In contrast, E-cadherin-deficient II-4 cells generated flattened groups of cells that were arrayed in a plexiform pattern (Fig. 6*a*, panel B), showing single cells that had detached from adjacent cells and migrated into the collagen gel (Fig. 6*a*, panel E). To determine the basis for differences in migratory behavior between E-cadherin-deficient and E-cadherin-competent cell lines, collagen gels were exposed for 4 days to GM-6001, a broad-spectrum MMP inhibitor, and the morphologic appearance of II-4 cells variants was compared. We found that exposure to GM-6001 blocked the migratory spread of H-2K^d-Ecad-expressing II-4 cells and reversed their morphology to that of rounded clusters (Fig. 6*b*, panel H). These clusters were very similar to GM-6001-treated H-2K^d-Ecad-ΔC25- (Fig. 6*b*, panels I and L) and pBabe-expressing (Fig. 6*b*, panels G and J) II-4 control cells. Interestingly, clusters of GM-6001-treated E-cadherin-deficient II-4 cells showed poor cell-cell adhesion and widened intercellular spaces (Fig. 6*b*, panel K), demonstrating that these cells

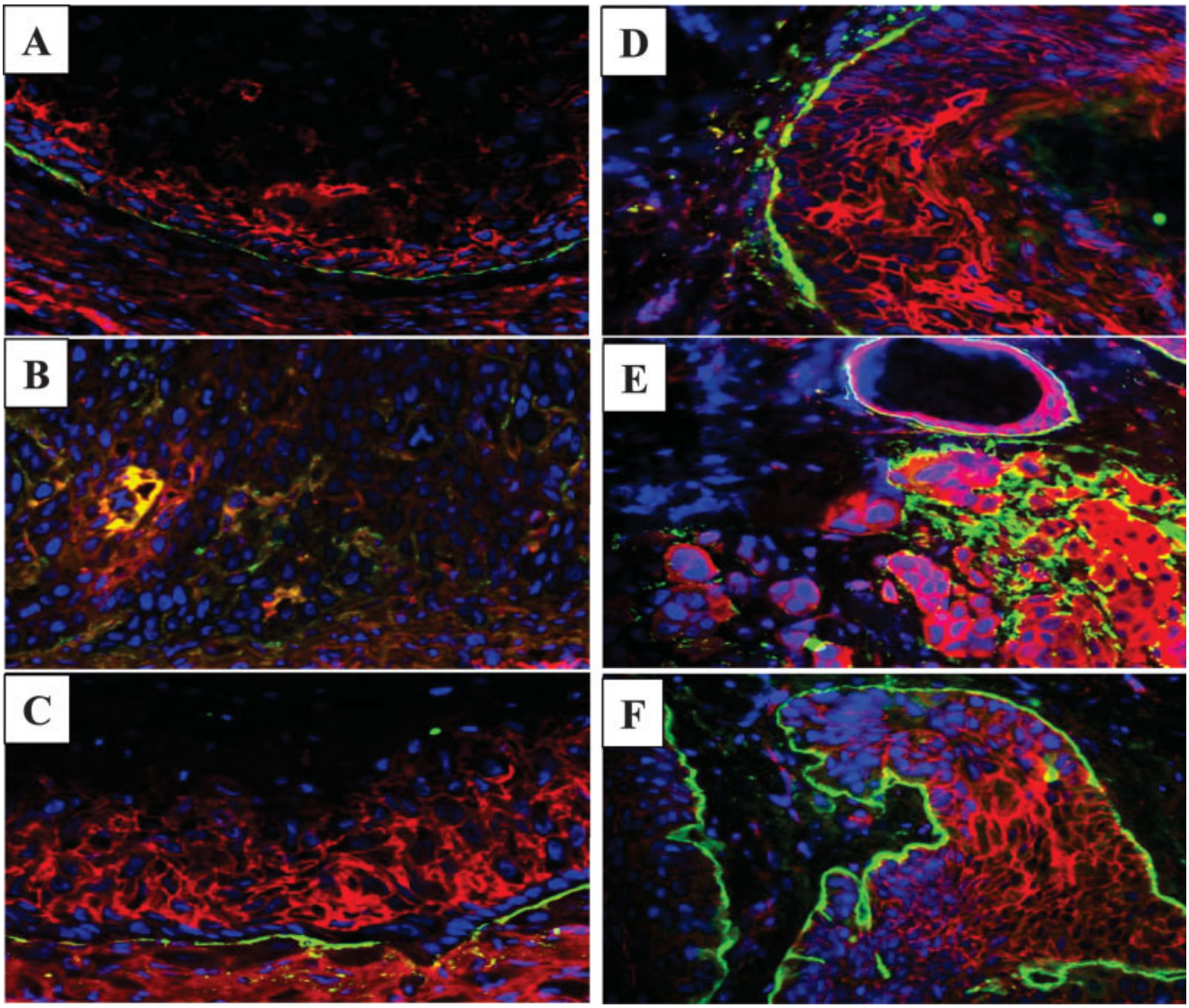

FIGURE 4 – Invasion of II-4 cells was associated with cytoplasmic redistribution of β-catenin, loss of endogenous E-cadherin and diffuse localization of the γ2 chain of laminin 5. Four-week-old transplants were analyzed by double immunofluorescence with antibodies against the γ2 chain of laminin 5 (FITC, green) and the extracellular domain of E-cadherin (*a–c*) or β-catenin (*d–f*; Texas Red, red). Highly aggressive H-2K^d-Ecad-expressing tumor cells exhibited diffuse pericellular localization of laminin 5 γ2 chain (*b*, yellow and *e*, green) as well as the cytoplasmic redistribution of β-catenin (*e*, red) and absence of endogenous E-cadherin staining (*b*). In contrast, control II-4 cells expressing pBabe and H-2K^d-EcadΔC25 exhibited linear staining for γ2 chain of laminin 5 at the periphery of tumor islands (*a*, *c*, *d* and *f*). Endogenous E-cadherin and β-catenin were localized at the borders of II-4 cells that expressed pBabe (*a* and *d*) and H-2K^d-EcadΔC25 (*c* and *f*). Note some background staining in the connective tissue (red) is seen in (*b*) adjacent to E-cadherin-negative tumor cells.

retained their nonadhesive phenotype in spite of losing their migratory properties. These findings demonstrated that activation of cell migration upon loss of E-cadherin was MMP-mediated.

To clarify the nature of this MMP-mediated activation, we performed function-blocking studies to determine if the migration of H-2K^d-expressing II-4 cells could be altered by more specific MMP inhibition. E-cadherin-deficient II-4 cells were seeded in collagen gels and grown in the presence of either TIMP-1 (200 ng/ml) or TIMP-2 (200 ng/ml) that was added to media 7 days after fabrication of collagen gels and maintained for 4 additional days. We observed that the presence of TIMP-2 reverted the morphology of E-cadherin-deficient cells to that of nonmigratory clusters (Fig. 6*c*) that were retained in rounded clusters and did not migrate into the surrounding collagen matrix and were similar to GM-6001-treated control II-4 cells (Fig. 6*c*). In contrast, when these E-cadherin-deficient II-4 cells were grown in the presence of TIMP-1, no inhibition of migration was seen (Fig. 6*c*). Under these conditions, individual II-4 cells migrated into the surrounding collagen in a pattern characteristic of nontreated control E-cadherin-deficient II-4 cells (Fig. 6*c*). These findings showed that E-cadherin-deficient II-4 cells were refractory to TIMP-1 yet sensitive to TIMP-2 inhibition of cell migration. Since MT1-MMP is known to be inhibited by TIMP-2 but not by TIMP-1, these functional blocking studies suggested that MT1-MMP was activated upon loss of E-cadherin and was linked to acquisition of the migratory behavior seen in collagen gels.

Loss of E-cadherin induces a switch to N-cadherin expression

To determine if loss of E-cadherin in II-4 cells was linked to the acquisition of cellular properties characteristic of epithelial-

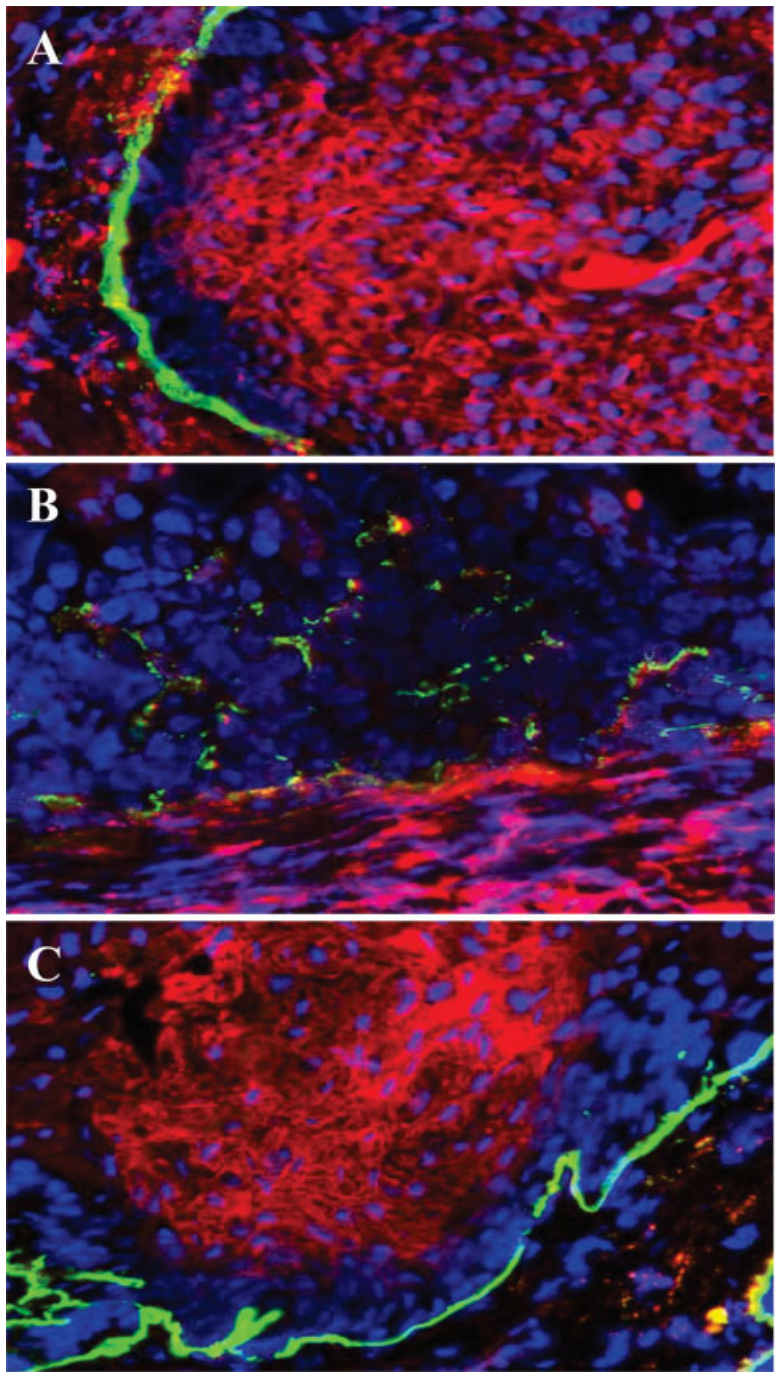

FIGURE 5 – Loss of keratin 1 expression was linked to loss of E-cadherin function. Sections from 4-week transplants of II-4 cells were analyzed by double immunofluorescence with an antibody directed against the epithelial differentiation marker cytokeratin 1 (K1) and γ2 chain of laminin 5. Keratin 1 was absent in II-4 cells that had lost E-cadherin function while diffuse deposition of γ2 chain of laminin 5 was seen between cells (*b*, green). In contrast, tumor islands expressing pBabe- (*a*) and H-2K^d-EcadΔC25 (*c*) were surrounded by linear deposition of γ2 chain of laminin 5 and showed expression of K1 in a stratum-specific manner.

mesenchymal transition (EMT), these cells and their E-cadherin-competent controls were analyzed to determine if expression of N-cadherin was elevated upon loss of E-cadherin. Analyses were performed for E-cadherin-competent and -deficient II-4 cells that were grown in 2D monolayer cultures (Fig. 7*a*), as well as for *in vitro* tissues generated by seeding cells into the 3D collagen gel migration assay. As seen by Western blot analysis of cellular lysates from 2D cultures, H-2K^d-Ecad-expressing II-4 cells demonstrated a significant upregulation of N-cadherin when compared to their pBabe-expressing and H-2K^d-Ecad-ΔC25-espressing controls (Fig. 7*a*). These findings were confirmed upon immunohistochemical stain of collagen gels for N-cadherin, where all E-cadherin-deficient cells demonstrated positive staining for N-cadherin (Fig. 7*b*, panel B). In contrast, E-cadherin-competent pBabe- and H-2K^d-Ecad-ΔC25-expressing control cells demonstrated only a small number of N-cadherin-positive cells (Fig. 7*b*, panels A and C). These findings demonstrated that cadherin subtype switching from E-cadherin to N-cadherin had occurred in E-cadherin-deficient II-4 cells. This switch may provide E-cadherin-deficient cells with enhanced migratory and invasive properties that were seen in 3D *in vitro* and *in vivo* assays.

Microarray analysis reveals genes differentially expressed upon loss of E-cadherin function in II-4 cells

We performed pairwise microarray analysis between H-2K^d-Ecad-expressing II-4 cells and their pBabe-expressing controls, to

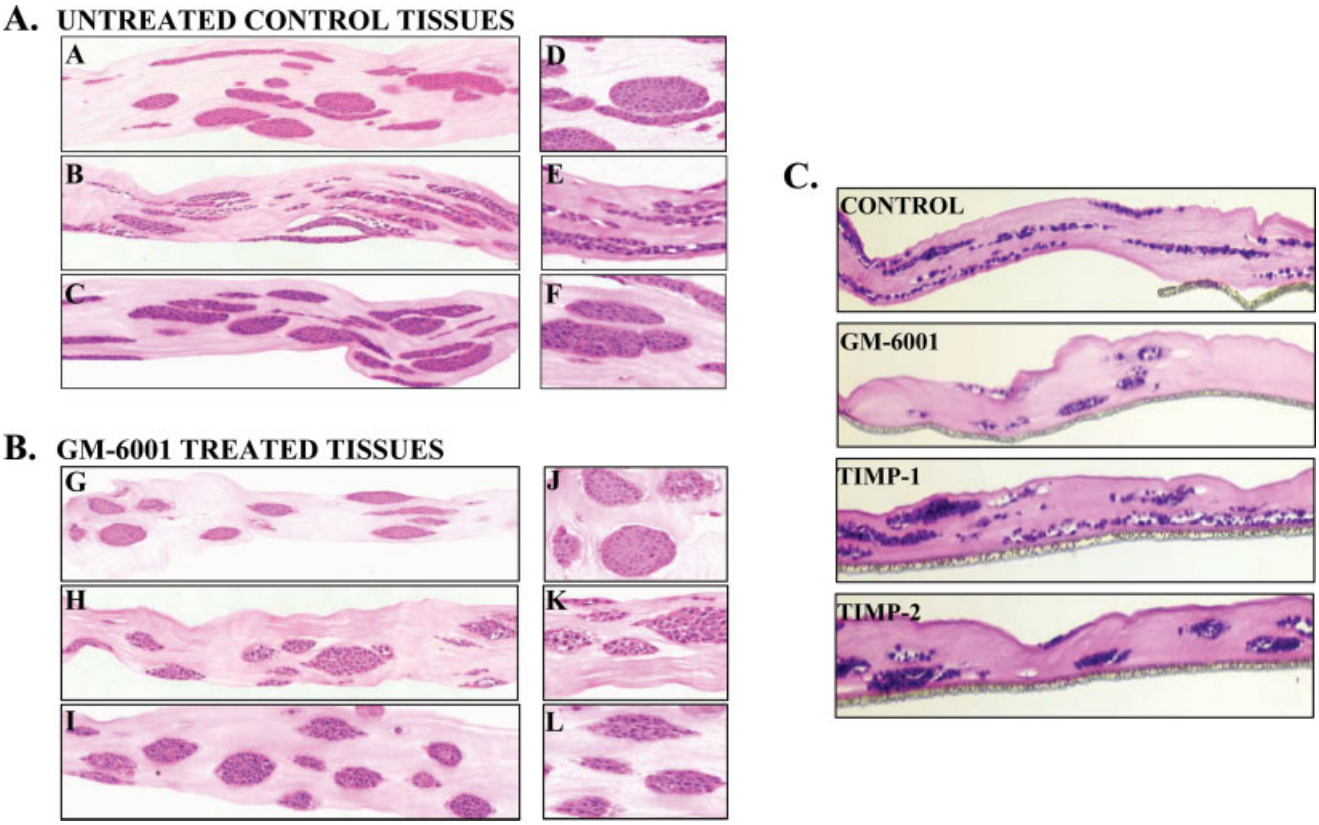

FIGURE 6 – E-cadherin-deficient cells activate MMP-mediated migration in 3D collagen gel migration assay. (*a*) E-cadherin competent pBabe- (panels A and D), H-2K^d-Ecad-ΔC25- (panels C and F) and E-cadherin-deficient H-2K^d-Ecad-expressing (panels B and E) cells were seeded into a type I collagen gel, grown for 11 days and stained with H&E to evaluate tissue morphology. E-cadherin-competent tissues showed clusters of cells that did not migrate into the surrounding collagen. In contrast, E-cadherin-deficient II-4 cells showed linear arrays of single cells that had detached from adjacent cells and underwent migration (panel E). Original magnification, 10× (panels A–C); 40× (panes D–F). (*b*) The migratory behavior of E-cadherin-deficient (panels H and K) and E-cadherin-competent cell lines (panels G, I, J and L) was compared in collagen gels when tissues were exposed to GM-6001 for the last 4 days of culture. GM-6001 blocked the migration of H-2K^d-Ecad-expressing II-4 cells (panel H) as seen by round clusters (panel K). These clusters were similar to GM-6001-treated H-2K^d-Ecad-ΔC25- (panels G and J) and pBabe-expressing (panels I and L) II-4 control cells. Original magnification, 10× (panels G–I); 40× (panels J–L). (*c*) E-cadherin-deficient II-4 cells were seeded into collagen gels (control) and grown in the presence of GM-6001, TIMP-1, or TIMP-2 for the last 4 days of culture. Cells in TIMP-2- and GM-6001-treated tissues did not migrate into the surrounding collagen matrix while cells in tissues exposed to TIMP-1 migrated and were similar to nontreated control E-cadherin-deficient II-4 cells. Original magnification, 10×.

compare their transcriptional profiles and identify candidate genes that may be associated with the switch to a high-grade tumor phenotype. Since we have found that the biologic behavior of the two E-cadherin-competent control cell lines, H-2K^d-Ecad-ΔC25 and pBabe, was identical after extensive characterization using *in vitro* and *in vivo* assays,[25] we used pBabe-expressing II-4 control cells for this comparative analysis of gene expression. We found genes whose expression was at least 2-fold greater in H-2K^d-Ecad-expressing II-4 cells than in pBabe-expressing cells. These include genes involved in cell cycle control whose expression may be linked to the elevated proliferation seen in E-cadherin-deficient tumors. Reflective of the highly invasive nature of H-2K^d-Ecad-expressing II-4 cells, proteases such as heparanase-like protein and ADAM12 were 4- and 7-fold elevated, respectively. In addition, proapoptotic molecules, including Bax and caspase-2, were elevated, as were kinases linked to PI3-K and MAPK pathways. Genes belonging to the *wnt*-signaling pathway, including the *wnt* receptor *frizzled* and its downstream target *disheveled*, were 3- to 5-fold elevated in E-cadherin-deficient cells and may be associated with the absence of differentiation in these tumors. Angiogenic growth factors such as vEGF-B and vEGF-C were elevated, as were genes that have been linked to the metastasis of squamous cell carcinoma, such as the chemokine receptor 4 (CXCR4). Finally, elevated expression of cell-cell and cell-matrix proteins was found in E-cadherin-deficient cells. In addition to proteins analyzed directly in excised tumors, these findings identify additional candidate genes and their associated pathways that may play a role in the activation of the aggressive phenotype seen upon loss of E-cadherin function.

Discussion

The cadherin family of adhesion molecules are known to link cell-cell adhesion with growth-signaling pathways and are therefore excellent molecular candidates to play a critical role in the regulation of cancer progression.[26] E-cadherin is known to function as a tumor suppressor gene during the advanced stages of cancer progression, where decreased expression of this protein has been associated with a poor clinical prognosis of several types of epithelial cancer.[4–6] However, little is known about the role that loss of E-cadherin may play in regulating the phenotypic properties of squamous cell carcinoma. To address this, we have directly determined how the loss of E-cadherin function could modify the tumorigenic properties and biologic behavior of squamous cell carcinoma cells. E-cadherin function was abrogated using a retro-

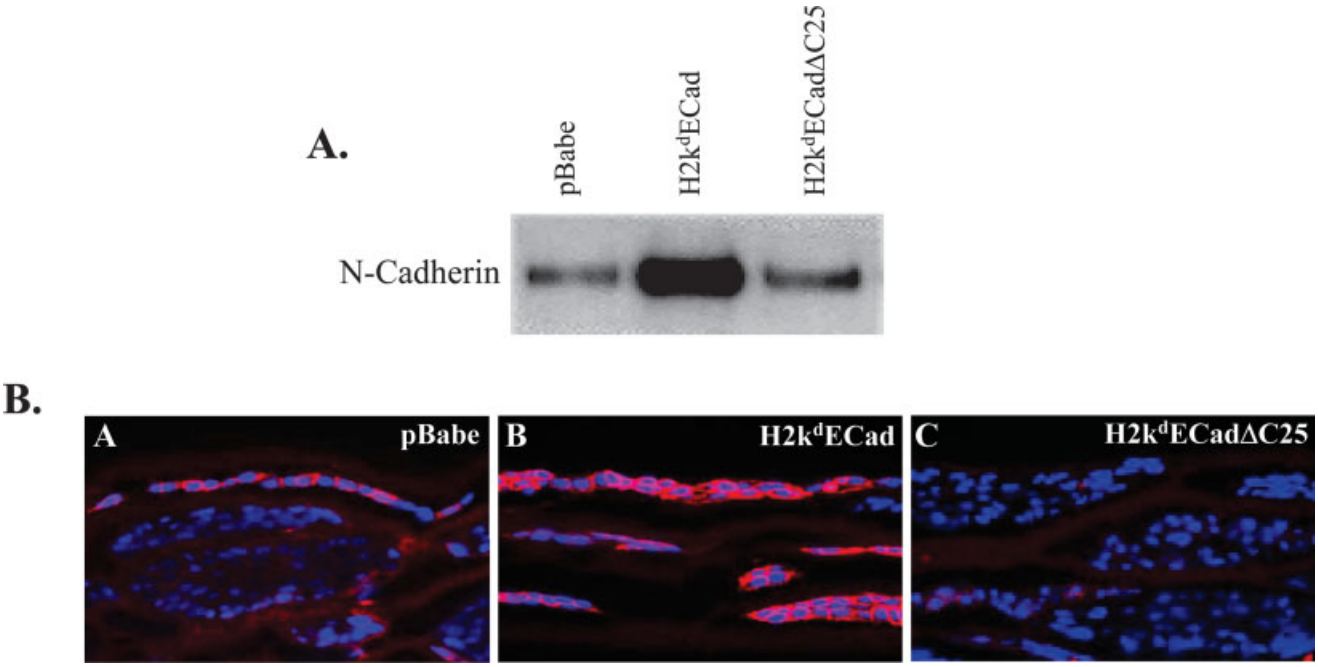

FIGURE 7 – Loss of E-cadherin induces a switch to N-cadherin expression. (*a*) Western blot analysis was used to analyze expression of N-cadherin in lysates from 2D cultures of II-4 cells expressing H-2K^d-Ecad (lane 2), pBabe (lane 1), or H-2K^d-Ecad-ΔC25 (lane 3). E-cadherin-deficient II-4 cells demonstrated a significant upregulation of N-cadherin when compared to controls. (*b*) Immunohistochemical stain for N-cadherin of cells in collagen gel migration assay. While E-cadherin-deficient cells demonstrated positive staining for N-cadherin in all cells (panel B), E-cadherin-competent pBabe- (panel A) and H-2K^d-Ecad-ΔC25- (panel C) expressing control cells demonstrated only small numbers of N-cadherin-positive cells. Original magnification, 10×.

viral vector encoding a dominant-negative mutant form of this protein and 3D human tissues that mimicked their *in vivo* counterparts were constructed to monitor the early stages of carcinoma progression. We found that loss of intercellular adhesion mediated by E-cadherin was sufficient to switch the biologic behavior of squamous cell carcinoma cells from low-grade, well-differentiated tumors to high-grade, poorly-differentiated carcinomas with a very aggressive phenotype. These studies provide the first direct evidence in human experimental 3D tissues that E-cadherin plays a critical role in regulating the cellular phenotype of invasive squamous carcinoma cells.

The induction of this highly aggressive form of carcinoma was associated with the emergence of rapidly proliferating, poorly differentiated tumor cells that demonstrated loss of cell-cell and cell-matrix adhesion proteins after *in vivo* transplantation. Elevated levels of tumor cell growth have previously been associated with the cytoplasmic redistribution of β-catenin in squamous cell carcinomas that were E-cadherin-deficient[27] and were linked to a considerably poorer survival rate. It is also known that loss of E-cadherin has been associated with a less differentiated phenotype of squamous cell carcinoma.[28–30] Altered expression of keratin genes characterized by the absence of high-molecular-weight keratins, such as K1, has previously been shown to be related to malignant growth properties.[31] The absence of keratin pearls and loss of K1 expression in tumors generated with E-cadherin-deficient II-4 cells confirmed this relationship between the concomitant loss of cell-cell adhesion and differentiation potential.[32]

Aberrant expression of the laminin 5 γ2 chain has been linked to the invasive behavior of several types of epithelial tumors. A diffuse pattern of immunohistochemical stain for γ2 chain has been associated with aggressive squamous cell carcinomas of the uterus and of the head and neck.[33,34] Similarly, elevated levels of γ2 chain[35] and abnormal patterns of laminin 5 degradation have been found in highly invasive SCC while a linear pattern of γ2 immunostain, similar to that seen in normal epithelia and in our control II-4 cells, has been described in mildly invasive SCC.[36] Other types of invasive tumors, such as gastric carcinoma,[37] are known to be associated with elevated expression of γ2 chain in areas of tumor cell budding, suggesting that this protein provides a migratory template to enable tumor cell invasion. The absence of staining for γ2 chain at the tumor cell-stroma interface has been previously reported in poorly differentiated SCC[38] and was similar to our findings at the leading edge of invading E-cadherin-deficient tumors. In light of these findings, it appears that the diffuse and poorly organized pericellular localization of γ2 chain suggests a role for laminin 5 that is distinct from its role in BM organization.[38] Additionally, the inability to form BM appears to be an important prognostic marker whose absence is associated with a more highly aggressive form of SCC. Altered expression of the laminin 5 γ2 chain is therefore a hallmark of highly invasive tumor cells that lack E-cadherin function. Thus, it appears that tumor cell phenotype and the stromal microenvironment work in concert to accelerate tumor cell invasion by deregulating the expression and organization of laminin 5.[39–41]

To elucidate the basis for differences seen in the pattern of invasion seen between E-cadherin-competent and E-cadherin-deficient II-4 cells after *in vivo* transplantation, we performed function blocking studies using natural (TIMP-1 and -2) and synthetic MMP inhibitors (GM6001) in a 3D collagen gel migration assay. We observed that E-cadherin-deficient cells did not spread into the surrounding collagen and formed stationary clusters when grown in the presence of an excess of GM6001 and TIMP-2, but were not inhibited by TIMP-1 treatment. Since MT1-MMP is known to be inhibited by TIMP-2 but not by TIMP-1, the refractory nature of E-cadherin-deficient cell clusters to TIMP-1 inhibition of migration suggested that activation of MT1-MMP was linked to the loss of E-cadherin and may partially explain acquisition of the more aggressive pattern of tumor cell invasion seen in E-cadherin-deficient II-4 cells. TIMP-2 has been shown to suppress MT1-MMP-mediated activation of pro-MMP-2 in II-4 cells grown in 2D monolayer cultures.[42] Similar responses to TIMP-1 and TIMP-2 have previously been reported to explain the migratory behavior

of endothelial cells,[43] breast cancer cells[44] and HT1080 cells[45] in collagen gels that has been linked to MT1-MMP-mediated proteolytic activity. In addition, our findings support the view that tumor cells embedded in collagen gels can retain their spherical shape in the absence of MT1-MMP-mediated proteolysis.[46] TIMP-1 has been shown to be a poor inhibitor of MT1-MMP,[47–51] while the presence of an excess of TIMP-2 can efficiently inhibit the collagenolytic activity of MT1-MMP by blocking the cleavage of pro-MMP-2 to the fully active form. After first demonstrating that migration of E-cadherin-deficient cells was MMP-mediated upon inhibition with the broad-spectrum MMP inhibitor GM-6001, we took advantage of these differential inhibitory properties of TIMP-1 and TIMP-2 to demonstrate that MT1-MMP is likely to play a role in the migration of E-cadherin-deficient cells.

Loss of E-cadherin function has been shown to trigger epithelial-mesenchymal transition that is associated with aggressive biologic behavior.[52,53] One aspect of this transition now includes the finding of an association between decreased E-cadherin expression and increased N-cadherin expression. As previously suggested, this cadherin switching may allow the acquisition of homophilic interactions between N-cadherin-expressing tumor cells and N-cadherin-expressing stromal cells, which may augment the invasive potential of carcinoma cells.[54] It has also been proposed that such interactions may provide a juxtacrine mechanism through which invading N-cadherin-positive tumor cells may induce the production of growth factors or proteases by stromal cells that may facilitate their invasive cells.[55] In this light, activation of N-cadherin expression may be viewed as a factor that modifies the tumor cell microenviroment to accelerate tumor cell invasion. Taken together with other findings, loss of E-cadherin activates a coordinated series of events that result in increased tumor cell growth, decreased tumor differentiation and enhancement of migratory and invasive properties that are mediated through altered tumor-stroma interactions.

Transcriptional profiles gleaned from microarray analysis demonstrated significant differences between H-2K^d-Ecad-expressing II-4 cells and pBabe-expressing controls that were consistent with the behavior of these tumors observed *in vivo*. These findings provide additional gene products that may be associated with the altered growth, differentiation, invasion and cell adhesion seen in E-cadherin-deficient tumors. The increased expression of cell-cell and cell-matrix proteins may be ascribed to the need of E-cadherin-deficient cells to synthesize alternative adhesive ligands upon activation of tumor cell migration. Surprisingly, H-2K^d-Ecad-expressing II-4 cells demonstrated elevated expression of proapoptotic molecules, including Bax and caspase-2. However, the function of these apoptotic markers may be overcome due to the overexpression of molecules active in survival-signaling cascades linked to PI3-K and MAPK pathways.[56] Genes in the *wnt*-signaling pathway, including the *wnt* receptor *frizzled* and its downstream target *disheveled*, were elevated 3- to 5-fold in E-cadherin-deficient cells and may be associated with the lack of differentiation of these tumors.[57] It is hoped that this overview of gene expression patterns will help identify new molecular markers that will be of prognostic value during the transition from low- to high-grade squamous cell carcinoma.

By generating 3D tissue constructs that mimic the *in vivo* tissue architecture of squamous cell carcinoma, this study provides a novel model to recapitulate the events that occur during tumorigenesis in human stratified squamous epithelium.[58] Since cell-cell adhesion is intimately related to organization of tissue architecture, the impact of its abrogation needs to be studied in such an appropriate 3D tissue context. Previous *in vivo* models designed to study the properties of invasive SCC have relied on heterotypic transplantation methods, such as subcutaneous injection of tumor cells, that do not accurately reflect epithelial tissue architecture during the initial stages of SCC progression in humans. The II-4 cell line used in our studies has been well characterized as a low-grade variant of squamous cell carcinoma.[16,21] Since these cells contain important genetic alterations that are commonly seen in SCC,[59] such as mutations in p53 and *ras*, they are particularly well suited for incorporation into 3D human tissue models of SCC progression by providing an appropriate genetic background to study how loss of E-cadherin function can further direct SCC progression. Taken together, our findings in a biologically meaningful 3D context show that a phenotypic switch, characterized by highly aggressive disseminated tumor cells, supports the view that the absence of E-cadherin is an important prognostic risk factor for the rapid progression of SCC. However, the nature of the molecular signals that direct this highly invasive tumor cell behavior remain to be elucidated.

Acknowledgements

The authors thank Ning Lin, Lina Nguyen and Robin Harrington for their technical assistance, Laura Bertolotti and Jennifer Landmann for their administrative assistance, Dr. F. Watt of the Imperial Cancer Research Center for the gift of the chimeric E-cadherin retroviral vectors and Dr. G. Meneguzzi for the laminin 5 antibody SE144.

References

1. Andrews NA, Jones AS, Helliwell TR, Kinsella AR. Expression of the E-cadherin-catenin cell adhesion complex in primary squamous cell carcinomas of the head and neck and their nodal metastases. Br J Cancer 1997;75:1474–80.
2. Behrens J. Cadherins and catenins: role in signal transduction and tumor progression. Cancer Metastasis Rev 1999;18:15–30.
3. Birchmeier W, Behrens J. Cadherin expression in carcinomas: role in the formation of cell junctions and the prevention of invasiveness. Biochim Biophys Acta 1994;1198:11–26.
4. Bagutti C, Speight PM, Watt FM. Comparison of integrin, cadherin, and catenin expression in squamous cell carcinomas of the oral cavity. J Pathol 1998;186:8–16.
5. Perl AK, Wilgenbus P, Dahl U, Semb H, Christofori G. A causal role for E-cadherin in the transition from adenoma to carcinoma. Nature 1998;392:190–3.
6. Yap AS. The morphogenetic role of cadherin cell adhesion molecules in human cancer: a thematic review. Cancer Invest 1998;16:252–61.
7. Behrens J, Mareel MM, Van Roy FM, Birchmeier W. Dissecting tumor cell invasion: epithelial cells acquire invasive properties after the loss of uvomorulin-mediated cell-cell adhesion. J Cell Biol 1989;108:2435–47.
8. Frixen UH, Behrens J, Sachs M, Eberle G, Voss B, Warda A, Lochner D, Birchmeier W. E-cadherin-mediated cell-cell adhesion prevents invasiveness of human carcinoma cells. J Cell Biol 1991;113:173–85.
9. Vleminckx K, Vakaet L Jr, Mareel M, Fiers W, Van Roy F. Genetic manipulation of E-cadherin expression by epithelial tumor cells reveals an invasion suppressor role. Cell 1991;66:107–19.
10. Noe V, Willems J, Vandekerckhove J, Roy FV, Bruyneel E, Mareel M. Inhibition of adhesion and induction of epithelial cell invasion by HAV-containing E-cadherin-specific peptides. J Cell Sci 1999;112(Pt 1):127–35.
11. Cano A, Gamallo C, Kemp CJ, Benito N, Palacios J, Quintanilla M, Balmain A. Expression pattern of the cell adhesion molecules. E-cadherin, P-cadherin and alpha 6 beta 4 intergrin is altered in pre-malignant skin tumors of p53-deficient mice. Int J Cancer 1996;65:254–62.
12. de Boer CJ, van Dorst E, van Krieken H, Jansen-van Rhijn CM, Warnaar SO, Fleuren GJ, Litvinov SV. Changing roles of cadherins and catenins during progression of squamous intraepithelial lesions in the uterine cervix. Am J Pathol 1999;155:505–15.
13. Bindels EM, Vermey M, van den Beemd R, Dinjens WN, Van Der Kwast TH. E-cadherin promotes intraepithelial expansion of bladder carcinoma cells in an *in vitro* model of carcinoma *in situ*. Cancer Res 2000;60:177–83.
14. Auersperg N, Pan J, Grove BD, Peterson T, Fisher J, Maines-Bandiera S, Somasiri A, Roskelley CD. E-cadherin induces mesenchymal-to-epithelial transition in human ovarian surface epithelium. Proc Natl Acad Sci USA 1999;96:6249–54.
15. Hagios C, Lochter A, Bissell MJ. Tissue architecture: the ultimate regulator of epithelial function? Philos Trans R Soc Lond B Biol Sci 1998;353:857–70.
16. Javaherian A, Vaccariello M, Fusenig NE, Garlick JA. Normal keratinocytes suppress early stages of neoplastic progression in stratified epithelium. Cancer Res 1998;58:2200–8.

17. Javaherian A, Fusenig NE, Vaccariello M, Garlick JA. A tissue model for premalignancy in stratified epithelium: bioengineering of skin substitutes. 1998.183–208.
18. Andriani F, Margulis A, Lin N, Griffey S, Garlick JA. Analysis of microenvironmental factors contributing to basement membrane assembly and normalized epidermal phenotype. J Invest Dermatol 2003;120:923–31.
19. Boukamp P, Breitkreutz D, Stark H-J, Fusenig NE. Mesenchyme-mediated and endogenous regulation of growth and differentiation of human skin keratinocytes derived from diffferent body sites. Differentiation 1990;44:150–61.
20. Boukamp P, Stanbridge EJ, Foo DY, Cerutti PA, Fusenig NE. c-Haras oncogene expression in immortalized human keratinocytes (HaCaT) alters growth potential *in vivo* but lacks correlation with malignancy. Cancer Res 1990;50:2840–7.
21. Fusenig NE, Boukamp P. Multiple stages and genetic alterations in immortalization, malignant transformation, and tumor progression of human skin keratinocytes. Mol Carcinogen 1998;23: 144–58.
22. Zhu AJ, Watt FM. Expression of a dominant negative cadherin mutant inhibits proliferation and stimulates terminal differentiation of human epidermal keratinocytes. J Cell Sci 1996;109:3013–23.
23. Margulis A, Andriani F, Fusenig N, Hashimoto K, Hanakawa Y, Garlick JA. Abrogation of E-cadherin-mediated adhesion induces tumor cell invasion in human skin-like organotypic cultures. J Invest Dermatol 2003;121:1182–90.
24. Vasioukhin V, Bauer C, Yin M, Fuchs E. Directed actin polymerization is the driving force for epithelial cell-cell adhesion. Cell 2000; 100:209–19.
25. Margulis A, Zhang W, Alt-Holland A, Crawford H, Fusenig N, Garlick J. E-cadherin suppression accelerates squamous cell carcinoma progression in 3D, human tissue constructs. Cancer Res 2005;65: 1783–91.
26. Bissell MJ, Radisky D. Putting tumours in context. Nat Rev Cancer 2001;1:46–54.
27. Papadavid E, Pignatelli M, Zakynthinos S, Krausz T, Chu AC. Abnormal immunoreactivity of the E-cadherin/catenin (alpha-, beta-, and gamma-) complex in premalignant and malignant non-melanocytic skin tumours. J Pathol 2002;196:154–62.
28. Sun W, Herrera GA. E-cadherin expression in invasive urothelial carcinoma. Ann Diagn Pathol 2004;8:17–22.
29. Behrendt GC, Hansmann ML. Carcinomas of the anal canal and anal margin differ in their expression of cadherin, cytokeratins and p53. Virch Arch 2001;439:782–6.
30. Wu H, Lotan R, Menter D, Lippman SM, Xu XC. Expression of E-cadherin is associated with squamous differentiation in squamous cell carcinomas. Anticancer Res 2000;20:1385–90.
31. Rheinwald JG, Beckett MA. Defective terminal differentiation in culture as a consistent and selectable character of malignant human keratinocytes. Cell 1980;22:629–32.
32. Wheelock MJ, Jensen PJ. Regulation of keratinocyte intercellular junction organization and epidermal morphogenesis by E-cadherin. J Cell Biol 1992;117:415–25.
33. Stoltzfus P, Salo S, Eriksson E, Aspenblad U, Tryggvason K, Auer G, Avall-Lundqvist E. Laminin-5 gamma2 chain expression facilitates detection of invasive squamous cell carcinoma of the uterine cervix. Int J Gynecol Pathol 2004;23:215–22.
34. Ono Y, Nakanishi Y, Gotoh M, Sakamoto M, Hirohashi S. Epidermal growth factor receptor gene amplification is correlated with laminin-5 gamma2 chain expression in oral squamous cell carcinoma cell lines. Cancer Lett 2002;175:197–204.
35. Pyke C, Romer J, Kallunki P, Lund LR, Ralfkiaer E, Dano K, Tryggvason K. The gamma 2 chain of kalinin/laminin 5 is preferentially expressed in invading malignant cells in human cancers. Am J Pathol 1994;145:782–91.
36. Shinohara M, Nakamura S, Harada T, Shimada M, Oka M. Mode of tumor invasion in oral squamous cell carcinoma: improved grading based on immunohistochemical examination of extracellular matrices. Head Neck 1996;18:153–9.
37. Pyke C, Salo S, Ralfkiaer E, Romer J, Dano K, Tryggvason K. Laminin-5 is a marker of invading cancer cells in some human carcinomas and is coexpressed with the receptor for urokinase plasminogen activator in budding cancer cells in colon adenocarcinomas. Cancer Res 1995;55:4132–9.
38. Patel V, Aldridge K, Ensley JF, Odell E, Boyd A, Jones J, Gutkind JS, Yeudall WA. Laminin-gamma2 overexpression in head-and-neck squamous cell carcinoma. Int J Cancer 2002;99:583–8.
39. Sordat I, Rousselle P, Chaubert P, Petermann O, Aberdam D, Bosman FT, Sordat B. Tumor cell budding and laminin-5 expression in colorectal carcinoma can be modulated by the tissue micro-environment. Int J Cancer 2000;88:708–17.
40. Sordat I, Bosman FT, Dorta G, Rousselle P, Aberdam D, Blum AL, Sordat B. Differential expression of laminin-5 subunits and integrin receptors in human colorectal neoplasia. J Pathol 1998;185:44–52.
41. Lohi J. Laminin-5 in the progression of carcinomas. Int J Cancer 2001;94:763–7.
42. Baumann P, Zigrino P, Mauch C, Breitkreutz D, Nischt R. Membrane-type 1 matrix metalloproteinase-mediated progelatinase A activation in non-tumorigenic and tumorigenic human keratinocytes. Br J Cancer 2000;83:1387–93.
43. Koike T, Vernon RB, Hamner MA, Sadoun E, Reed MJ. MT1-MMP, but not secreted MMPs, influences the migration of human microvascular endothelial cells in 3-dimensional collagen gels. J Cell Biochem 2002;86:748–58.
44. Koshikawa N, Giannelli G, Cirulli V, Miyazaki K, Quaranta V. Role of cell surface metalloprotease MT1-MMP in epithelial cell migration over laminin-5. J Cell Biol 2000;148:615–24.
45. Takino T, Miyamori H, Watanabe Y, Yoshioka K, Seiki M, Sato H. Membrane type 1 matrix metalloproteinase regulates collagen-dependent mitogen-activated protein/extracellular signal-related kinase activation and cell migration. Cancer Res 2004;64:1044–9.
46. Hotary KB, Allen ED, Brooks PC, Datta NS, Long MW, Weiss SJ. Membrane type I matrix metalloproteinase usurps tumor growth control imposed by the three-dimensional extracellular matrix. Cell 2003;114:33–45.
47. D'Ortho MP, Stanton H, Butler M, Atkinson SJ, Murphy G, Hembry RM. MT1-MMP on the cell surface causes focal degradation of gelatin films. FEBS Lett 1998;421:159–64.
48. Atkinson SJ, Crabbe T, Cowell S, Ward RV, Butler MJ, Sato H, Seiki M, Reynolds JJ, Murphy G. Intermolecular autolytic cleavage can contribute to the activation of progelatinase A by cell membranes. J Biol Chem 1995;270:30479–85.
49. Will H, Atkinson SJ, Butler GS, Smith B, Murphy G. The soluble catalytic domain of membrane type 1 matrix metalloproteinase cleaves the propeptide of progelatinase A and initiates autoproteolytic activation: regulation by TIMP-2 and TIMP-3. J Biol Chem 1996;271:17119–23.
50. Lichte A, Kolkenbrock H, Tschesche H. The recombinant catalytic domain of membrane-type matrix metalloproteinase-1 (MT1-MMP) induces activation of progelatinase A and progelatinase A complexed with TIMP-2. FEBS Lett 1996;397:277–82.
51. Butler GS, Butler MJ, Atkinson SJ, Will H, Tamura T, van Westrum SS, Crabbe T, Clements J, D'Ortho MP, Murphy G. The TIMP2 membrane type 1 metalloproteinase ''receptor'' regulates the concentration and efficient activation of progelatinase A: a kinetic study. J Biol Chem 1998;273:871–80.
52. Egeblad M, Werb Z. New functions for the matrix metalloproteinases in cancer progression. Nat Rev Cancer 2002;2:161–74.
53. Boukamp P, Fusenig NE. ''Trans-differentiation'' from epidermal to mesenchymal/myogenic phenotype is associated with a drastic change in cell-cell and cell-matrix adhesion molecules. J Cell Biol 1993; 120:981–93.
54. Hazan RB, Qiao R, Keren R, Badano I, Suyama K. Cadherin switch in tumor progression. Ann NY Acad Sci 2004;1014:155–63.
55. Li G, Satyamoorthy K, Herlyn M. N-cadherin-mediated intercellular interactions promote survival and migration of melanoma cells. Cancer Res 2001;61:3819–25.
56. Granville DJ, Carthy CM, Hunt DW, McManus BM. Apoptosis: molecular aspects of cell death and disease. Lab Invest 1998;78:893–913.
57. Shelly LL, Fuchs C, Miele L. Notch-1 inhibits apoptosis in murine erythroleukemia cells and is necessary for differentiation induced by hybrid polar compounds. J Cell Biochem 1999;73:164–75.
58. Takahashi M, Fujita M, Furukawa Y, Hamamoto R, Shimokawa T, Miwa N, Ogawa M, Nakamura Y. Isolation of a novel human gene, *APCDD1*, as a direct target of the beta-catenin/T-cell factor 4 complex with probable involvement in colorectal carcinogenesis. Cancer Res 2002;62.
59. Dlugosz A, Merlino G, Yuspa SH. Progress in cutaneous cancer research. J Invest Dermatol Symp Proc 2002;7:17–26.

gibco

24 days of stem cells

Shape the future of stem cell innovation

October 1- November 1, 2019

Join us for 24 Days of Stem Cells; a premiere virtual event featuring the latest advances in stem cell research.

This year's format will feature a new hour of cutting edge content every week day starting October 1st. Attend the sessions that are most relevant to your work - at your convenience and at your pace.

During the 24-day long event, you can:

- Access leading scientific presentations from thought leaders around the world
- Watch live training demonstrations from our stem cell experts
- Download key stem cell tools and resources
- Complete weekly challenges to earn points towards certification and prizes

Register today at
www.24daysofstemcells.com

ThermoFisher SCIENTIFIC

WILEY